Secondary Electron Emission from a Negatively Charged Spherical Dust Particle by Electron Incidence*)

Yukihiro TOMITA, Gakushi KAWAMURA, Zhihui HUANG[1)], Yudong PAN[1)] and Longwen YAN[1)]

National Institute for Fusion Science, 322-6 Oroshi-cho, Toki 509-5292, Japan

[1)]*Southwestern Institute of Physics, P.O. Box 432, Chengdu 610041, Sichuan, China*

(Received 22 November 2012 / Accepted 8 March 2013)

Secondary electron emission (SEE) from a spherical metallic dust particle by electron incidence was analyzed according to the OML (Orbit Motion Limited) model. As the observed dust speed in fusion plasmas (< 100 m/s) is much slower than electron thermal speed, its effect to the SEE current is negligibly small. It is clarified that there is a window of electron temperature, where the ratio of the SEE current to the absorbed electron current exceeds unity; for graphite 80 eV < T_e < 326 eV and the maximum of the ratio ~ 1.10 at T_e ~ 165 eV, for tungsten 32 eV < T_e, the maximum ~ 2.47 at T_e ~ 358 eV. These excesses come from the inverse proportion of the incident angle to the dust particle.

Keywords: dust particle, secondary electron emission, electron impact, dust charge

DOI: 10.1585/pfr.8.2401028

1. Introduction

The behavior of dust particles in fusion plasmas is one of the interesting subjects as well as in the astrophysical, space, laboratory, and processing plasmas. In present fusion plasmas the characteristics of dust particles have been analyzed, where the dust radii are varied from 10 nm to 100 μm with the spherical and flake shapes [1–3]. Their main components were carbon and constituents of stainless steel (SS), which are used for divertor plates and most plasma-facing components (PFC). One of the particular subjects in fusion devices is associated with absorption of radioactive tritium [4]. For these objectives the dynamics of the dust particle in fusion plasma is extensively studied [5–7]. In order to analyze the dust dynamics in plasmas, the dust charge state decides its dynamics, which is investigated according to the OML model [8, 9]. The secondary electron emission (SEE), however, is introduced by the simple model, where the incident angle has a cosine distribution from the surface normal of the dust particle [6, 7]. In this study we investigate the exact incident angle according to the OML model and obtain the SEE current from the dust particle with spherical shape.

2. Emission Due to Electron Incidence

The incident quantities, such as energy and angle, of an electron to the spherical dust surface with a radius R_d are obtained according to the OML theory, where the energy and angular momentum of an electron are conserved. The relation between an incident energy E_{inc} and an impact energy E_0 is expressed as:

$$E_{inc} = E_0 - \psi_{Rd}. \tag{1}$$

Here $\psi_{Rd} = Z_d e^2/4\pi\varepsilon_0 R_d$ is the potential energy at the dust surface, where Z_d (> 0) is the dust charge state. The dust particle in relatively low temperature plasmas at SOL/divertor region is negatively charged due to the high mobility of plasma electrons. The electron with the lower energy than the potential energy ψ_{Rd} is reflected and does not reach to the dust surface. The incident angle θ_{inc} from the surface normal of the dust is obtained:

$$\theta_{inc} = \arctan \frac{\lambda_0}{\sqrt{1 - \lambda_0^2 - \beta_0}}, \tag{2}$$

where $\lambda_0 = \rho_0/R_d$ is the normalized impact parameter ρ_0 by the dust radius R_d and $\beta_0 = \psi_{Rd}/E_0$. By using these relations the rate of an emitted number due to the electron incidence is obtained as:

$$G_{emt} = 2\pi n_e \int_{u_{0,min}}^{\infty} d\vec{u}_0 u_0 f_e(\vec{u}_0 + \vec{V}_d) \int_0^{\rho_{0,max}(u_0)} d\rho_0 \rho_0 Y_{emt}(E_{inc}, \theta_{inc}), \tag{3}$$

where $\vec{u}_0 (= \vec{v}_0 - \vec{V}_d)$ is the relative velocity of an electron velocity $\vec{v}_0$ to the dust velocity $\vec{V}_d$. The impact electron velocity distribution function and density are indicated by f_e and n_e, respectively. The quantity Y_{emt} is the emission yield. The minimum relative speed $u_{0,min}$ =

author's e-mail: tomita@nifs.ac.jp

*) This article is based on the presentation at the 22nd International Toki Conference (ITC22).

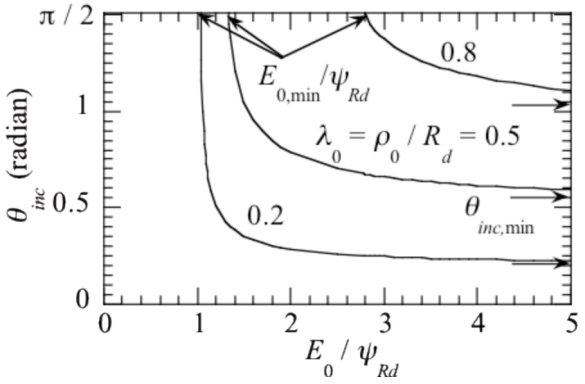

Fig. 1 Relation between an impact energy E_0 and an incident angle $\theta_{\rm inc}$ in the cases $\lambda_0 = \rho_0/R_{\rm d} = 0.2$, 0.5 and 0.8.

$\sqrt{2\psi_{\rm Rd}/m_{\rm e}}$. The maximum of the impact parameter $\rho_{0,\max}$ is $R_{\rm d}\sqrt{1-\beta_0}$, where electrons with the larger impact parameter than $\rho_{0,\max}$ are reflected and pass through the dust without incidence. In Fig. 1 the incident angle $\theta_{\rm inc}$ is shown as a function of the normalized impact energy E_0 by $\psi_{\rm Rd}$, where the normalized impact parameters $\rho_0/R_{\rm d}$ are 0.2, 0.5 and 0.8. The minimum of normalized impact energy is $E_{0,\min}/\psi_{\rm Rd} = 1/[1-(\rho_0/R_{\rm d})^2]$ for each normalized impact parameter, where an electron injects tangentially, $\theta_{\rm inc} = \pi/2$. The minimum incident angle, where the impact electron energy is infinity, is $\theta_{\rm inc,min} = \arctan[(\rho_0/R_{\rm d})/\sqrt{1-(\rho_0/R_{\rm d})^2}]$. The quantities of $E_{0,\min}/\psi_{\rm Rd}$ and $\theta_{\rm inc,min}$ for each case are indicated by arrows in Fig. 1.

3. Secondary Electron Emission

The equilibrium dust charge in plasmas is decided by the floating condition, where the electron current is equal to the ion current to the dust particle [10]. By using this condition under the OML model without the SEE current, the parameter of the equilibrium charge $Z_{\rm d,eq}/R_{\rm d}T_{\rm e}$ is obtained as a function of relative speed of plasma ion flow to the dust speed and the plasma temperature ratio $T_{\rm i}/T_{\rm e}$. For the typical SOL/divertor plasma, where the dust speed is much slower than the ion flow speed, the equilibrium dust charge state is around $Z_{\rm d,eq} = 2\times10^5$ in the case of $T_{\rm e} = 100\,{\rm eV}$ and $R_{\rm d} = 1\,\mu{\rm m}$.

The empirical formula of the SEE yield $Y_{\rm see}$ is described as a function of an incident energy $E_{\rm inc}$, Kollath's formula [11], and an incident angle $\theta_{\rm inc}$ as:

$$Y_{\rm see}(E_{\rm inc},\theta_{\rm inc}) = \delta_{\rm m}\frac{E_{\rm inc}}{E_{\rm m}}\exp\left[-2\left(\sqrt{\frac{E_{\rm inc}}{E_{\rm m}}}-1\right)\right](\cos\theta_{\rm inc})^{\alpha}. \quad (4)$$

Here $\delta_{\rm m}$ is the value of the SEE yield at maximum for the normal incidence ($\theta_{\rm inc} = \pi/2$), $E_{\rm m}$ is the energy of incident electron corresponding to the maximum yield. The factor α is -1.0 for the materials of high nuclear charge. For graphite $\delta_{\rm m} = 1.0$, $E_{\rm m} = 300\,{\rm eV}$ and $\alpha = -0.4$ [12]. For tungsten $\delta_{\rm m} = 1.4$, $E_{\rm m} = 650\,{\rm eV}$ and $\alpha = -1.0$.

In the case of the Maxwell electron velocity distribution, the SEE current is obtained in the next sub-section.

3.1 Secondary electron emission current: $V_{\rm d} = 0$

The dust speed observed in plasmas of the present fusion experiments is around few tens m/sec, which is much slower than the electron thermal speed. The secondary electron emission current with $V_{\rm d} = 0$ is calculated as:

$$I_{\rm see,Vd=0} = \frac{2}{\sqrt{\pi}}e\pi R_{\rm d}^2 n_{\rm e}\upsilon_{\rm the}\frac{2.72^2\delta_{\rm m}}{(2+\alpha)E_{\rm m}/T_{\rm e}} g_{\rm see,Vd=0}\left(\frac{\psi_{\rm Rd}}{T_{\rm e}},\frac{T_{\rm e}}{E_{\rm m}}\right), \quad (5)$$

where

$$g_{\rm see,Vd=0}\left(\frac{\psi_{\rm Rd}}{T_{\rm e}},\frac{T_{\rm e}}{E_{\rm m}}\right) = e^{-\psi_{\rm Rd}/T_{\rm e}}\left[2\delta^4+9\delta^2+4 -\frac{\sqrt{\pi}}{2}(4\delta^5+20\delta^3+15\delta)e^{\delta^2}\,{\rm erfc}\,\delta\right], \quad (6)$$

and $\upsilon_{\rm the} = \sqrt{2T_{\rm e}/m_{\rm e}}$, $\delta = \sqrt{T_{\rm e}/E_{\rm m}}$ and erfc δ is the complimentary error function. The incident electron current, which is absorbed current to the dust $I_{\rm abs,Vd=0}$, is obtained as $Y_{\rm emt}(\varepsilon_{\rm inc},\theta_{\rm inc}) = 1$ in the SEE current Eq. (3):

$$I_{\rm abs,Vd=0} = e\pi R_{\rm d}^2 n_{\rm e}\sqrt{\frac{2T_{\rm e}}{m_{\rm e}}}\frac{2}{\sqrt{\pi}}e^{-\psi_{\rm Rd}/T_{\rm e}}. \quad (7)$$

These give us the ratio of the SEE current to the absorbed current $\gamma_{\rm see,Vd=0}$, which depends on the SEE parameters, such as $\delta_{\rm m}, E_{\rm m}$ and α, and the electron temperature $T_{\rm e}$, it is, however, independent of the dust charge $Z_{\rm d}$ as well as the dust radius $R_{\rm d}$.

$$\gamma_{\rm see,Vd=0} = \frac{2.72^2\delta_{\rm m}}{2+\alpha}\eta_{\rm see,Vd=0}\left(\frac{T_{\rm e}}{E_{\rm m}}\right), \quad (8)$$

where

$$\eta_{\rm see,Vd=0}(T_{\rm e}/E_{\rm m}) = \delta^2\left[2\delta^4+9\delta^2+4-\frac{\sqrt{\pi}}{2}(4\delta^5+20\delta^3+15\delta)e^{\delta^2}\,{\rm erfc}\,\delta\right]. \quad (9)$$

In Fig. 2 the function $\eta_{\rm see,Vd=0}$ is shown as a function of $T_{\rm e}/E_{\rm m}$, where the function $\eta_{\rm see,Vd=0}$ has a maximum of 0.239 at $T_{\rm e}/E_{\rm m} = 0.552$.

In Fig. 3 the ratios of the SEE current $\gamma_{\rm see,Vd=0}$ are shown in the cases of (*a*) carbon (graphite: $\delta_{\rm m} = 1.0$, $E_{\rm m.} = 300\,{\rm eV}$, $\alpha = -0.4$) and (*b*) tungsten ($\delta_{\rm m} = 1.4$, $E_{\rm m.} = 650\,{\rm eV}$, $\alpha = -1.0$), where the cases of $\alpha = 0$, which correspond to the normal incidence, are also shown. For carbon though the maximum of the ratio is less than unity for the normal incidence ($\alpha = 0$), that with $\alpha = -0.4$ exceeds unity because of the inverse proportion of cos $\theta_{\rm inc}$

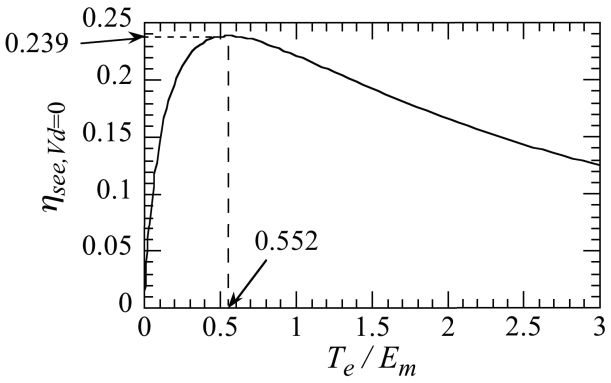

Fig. 2 Plasma temperature dependence of the function $\eta_{\mathrm{see,Vd=0}}$, where there is a maximum of 0.239 at $T_\mathrm{e}/E_\mathrm{m} = 0.552$.

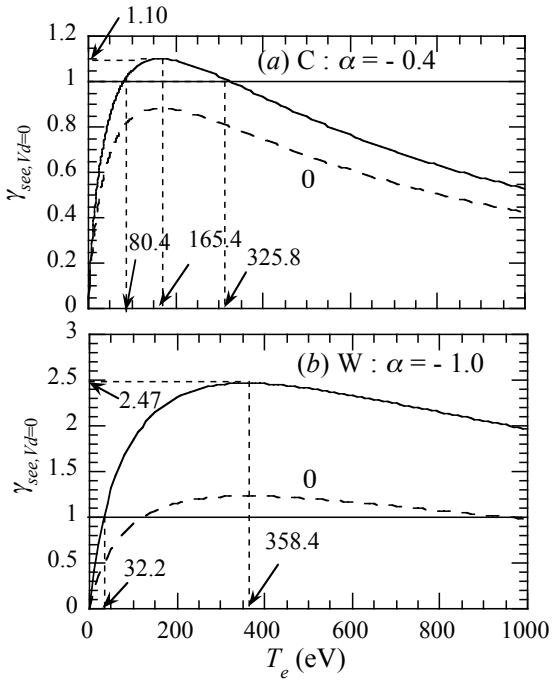

Fig. 3 Ratios of SEE current $\gamma_{\mathrm{see,Vd>0}}$ in the cases of (*a*) C (graphite: $\delta_\mathrm{m} = 1.0$, $E_\mathrm{m.} = 300\,\mathrm{eV}$, $\alpha = -0.4$) and (*b*) W ($\delta_\mathrm{m} = 1.4$, $E_\mathrm{m.} = 650\,\mathrm{eV}$, $\alpha = -1.0$), where the cases of $\alpha = 0$ are also shown by dashed lines.

to the SEE yield. For tungsten even the normal incidence ($\alpha = 0$) the maximum value is larger than unity, which comes from the large maximum yield ($\delta_\mathrm{m} = 1.4$). The inverse proportion of $\cos\theta_\mathrm{inc}$ ($\alpha = -1.0$) enhances the maximum of the ratio $\gamma_{\mathrm{see,Vd=0}}$ compared to the case of graphite ($\alpha = -0.4$). For both cases there is a window of electron temperature, where the ratio $\gamma_{\mathrm{see,Vd=0}}$ exceeds unity for graphite $80\,\mathrm{eV} < T_\mathrm{e} < 326\,\mathrm{eV}$ and the maximum of the ratio ~ 1.10 at $T_\mathrm{e} \sim 165\,\mathrm{eV}$, for tungsten $32\,\mathrm{eV} < T_\mathrm{e}$, the maximum ~ 2.47 at $T_\mathrm{e} \sim 358\,\mathrm{eV}$.

3.2 Secondary electron emission current: effect of dust speed

The effect of the finite dust speed is investigated in this section. The secondary electron emission current with the finite dust speed is expressed as:

$$I_{\mathrm{see,Vd>0}} = \frac{2}{\sqrt{\pi}} e\pi R_\mathrm{d}^2 n_\mathrm{e} \upsilon_\mathrm{the} \frac{2.72^2 \delta_\mathrm{m}}{(2+\alpha)E_\mathrm{m}/T_\mathrm{e}} g_{\mathrm{see,Vd>0}}(T_\mathrm{e}, \bar{\psi}_\mathrm{Rd}, \bar{V}_\mathrm{d}), \tag{10}$$

where

$$\begin{cases} g_{\mathrm{see,Vd>0}}(T_\mathrm{e}, \bar{\psi}_\mathrm{Rd}, \bar{V}_\mathrm{d}) \\ \quad \equiv \dfrac{1}{\bar{V}_\mathrm{d}} \displaystyle\int_{w_\mathrm{min}}^{\infty} dw (w^2 - \bar{\psi}_\mathrm{Rd})^2 e^{-2\sqrt{T_\mathrm{e}/E_\mathrm{m}}\sqrt{w^2-\bar{\psi}_\mathrm{Rd}}} \\ \qquad\qquad [e^{-(w-\bar{V}_\mathrm{d})^2} - e^{-(w+\bar{V}_\mathrm{d})^2}] \\ w_\mathrm{min} = \sqrt{\bar{\psi}_\mathrm{Rd}}, \bar{\psi}_\mathrm{Rd} = \psi_\mathrm{Rd}/T_\mathrm{e}, \bar{V}_\mathrm{d} = V_\mathrm{d}/\sqrt{2T_\mathrm{e}/m_\mathrm{e}}. \end{cases} \tag{11}$$

The absorbed current with finite dust speed $I_{\mathrm{abs,Vd>0}}$ is

$$I_{\mathrm{abs,Vd>0}} = \frac{2}{\sqrt{\pi}} e\pi R_\mathrm{d}^2 n_\mathrm{e} \upsilon_\mathrm{the} g_{\mathrm{abs,Vd>0}}(T_\mathrm{e}, \bar{\psi}_\mathrm{Rd}, \bar{V}_\mathrm{d}), \tag{12}$$

where

$$g_{\mathrm{abs,Vd>0}}(T_\mathrm{e}, \bar{\psi}_\mathrm{Rd}, \bar{V}_\mathrm{d}) = \frac{\sqrt{\pi}}{8\bar{V}_\mathrm{d}} \left[\frac{2}{\sqrt{\pi}} (w_p e^{-w_\mathrm{m}^2} - w_\mathrm{m} e^{-w_p^2}) + (1 + 2\bar{V}_\mathrm{d}^2 - 2\bar{\psi}_\mathrm{Rd})(\mathrm{erf}\, w_\mathrm{p} - \mathrm{erf}\, w_\mathrm{m}) \right], \tag{13}$$

and $w_\mathrm{m} = \sqrt{\bar{\psi}_\mathrm{Rd}} - \bar{V}_\mathrm{d}, w_\mathrm{p} = \sqrt{\bar{\psi}_\mathrm{Rd}} + \bar{V}_\mathrm{d}$. The ratio of the SEE current $\gamma_{\mathrm{abs,Vd>0}}$ is obtained as:

$$\gamma_{\mathrm{see,Vd>0}} = \frac{2.72^2 \delta_\mathrm{m}}{2+\alpha} \frac{T_\mathrm{e}}{E_\mathrm{m}} \frac{g_{\mathrm{see,Vd>0}}(T_\mathrm{e}, \bar{\psi}_\mathrm{Rd}, \bar{V}_\mathrm{d})}{g_{\mathrm{abs,Vd>0}}(T_\mathrm{e}, \bar{\psi}_\mathrm{Rd}, \bar{V}_\mathrm{d})}. \tag{14}$$

The normalized difference from $V_\mathrm{d} = 0$ $(\gamma_{\mathrm{see,Vd>0}} - \gamma_{\mathrm{see,Vd=0}})/\gamma_{\mathrm{see,Vd=0}}$ is shown in Fig. 4 for the $T_\mathrm{e} = 10\,\mathrm{eV}$.

This result indicates the effect of the dust speed to be negligibly small because the observed dust speed is much smaller than the electron thermal speed.

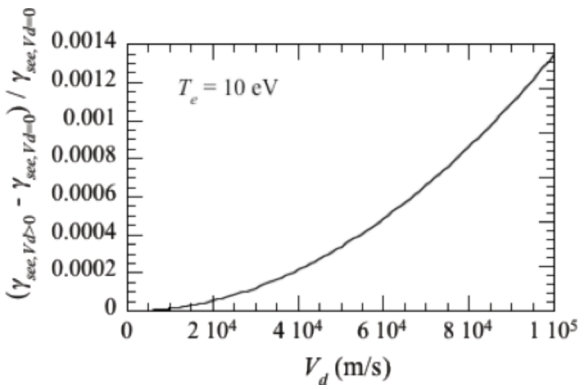

Fig. 4 Difference of ratio between $\gamma_{\mathrm{see,Vd>0}}$ and $\gamma_{\mathrm{see,Vd=0}}$ as a function of dust speed V_d.

4. Summary

The secondary electron emission was investigated according to OML model for a spherical metallic dust particle. As the dust speed (< 100 m/s) is much slower than the electron thermal speed, the effect of the finite dust speed is negligibly small to the SEE current. In the case of the zero dust speed, it is clarified that there is a window of electron temperature, where the ratio $\gamma_{\rm see}$ exceeds unity for graphite 80 eV < $T_{\rm e}$ < 326 eV and the maximum of the ratio ~ 1.10 at $T_{\rm e}$ ~ 165 eV, for tungsten 32 eV < $T_{\rm e}$, the maximum ~ 2.47 at $T_{\rm e}$ ~ 358 eV. The larger SEE current than unity makes the shallower potential drop of the dust particle to decrease the ion current under the floating condition of the dust in plasmas. The decrease of ion flux to the dust may reduce the ion friction force and the heat load to the dust. Furthermore, there is a possibility for the larger SEE current to make the dust charge positive.

The following issues are remained as future studies: (i) other emissions like SEE due to ion bombardment, backscattering of electrons and ions, thermal emission, etc. (ii) equilibrium charge of floating dust including the SEE, (iii) effects of SEE to forces on a dust and dynamics in fusion plasmas. One of the important issues is cross-validation of the charging model of the dust and experiments.

Acknowledgements

This work is partly supported by the National Magnetic Confinement Fusion Science Program of China (No. 2009GB106006)

[1] J. Winter, Plasma Phys. Control. Fusion **40**, 1201 (1998).
[2] A. Sagara, S. Masuzaki, T. Morisaki *et al.*, J. Nucl. Mater. **313-316**, 1 (2003).
[3] J. Sharpe, V. Rohde, The ASDEX-U Experiment Team *et al.*, J. Nucl. Mater. **313-316**, 455 (2003).
[4] J. Winter, Plasma Phys. Control. Fusion **46**, B583 (2004).
[5] S. Krasheninnikov, Y. Tomita, R. Smirnov and R. Janev, Phys. Plasma **11**, 3141 (2004).
[6] A. Pigarov, S. Krasheninnikov, T. Soboleva and T. Rognlien, Phys. Plasma **12**, 122508 (2005).
[7] R. Smirnov, A. Pigarov, M. Rosenberg *et al.*, Plasma Phys. Control. Fusion **49**, 347 (2007).
[8] H. Mott-Smith and I. Langmuir, Phys. Rev. **28**, 727 (1926).
[9] J. Allen, Phisica Scripta **45**, 497 (1992).
[10] Y. Tomita, G. Kawamura, Z.H. Huang, Y.D. Pan and L.W. Yan, Plasma Sci. Technol. **13**, 11 (2011).
[11] E.W. Thomas, Data Compendium for Plasma-Surface Interaction (Vienna: IAEA) p.94.
[12] J.M. Pedgley and G.M. McCracken, Plasma Phys. Control. Fusion **35**, 397 (1993).